Biosystems Engineering (2002) **83** (2), 129–147
doi:10.1016/S1537-5110(02)00172-1, available online at http://www.idealibrary.com on IDEAL®
SE—Structures and Environment

REVIEW PAPER

Convective and Ventilation Transfers in Greenhouses, Part 2: Determination of the Distributed Greenhouse Climate

T. Boulard[1]; C. Kittas[2]; J.C. Roy[3]; S. Wang[4]

[1] INRA, Unité Plantes et Systèmes de Culture Horticoles, Domaine St Paul, Site Agroparc, 84914 Avignon Cedex 09, France; e-mail of corresponding author: boulard@avignon.inra.fr
[2] School of Agriculture, University of Thessaly, Phytokou Street, 38446 N. Ionia Magnisias, Greece; e-mail:ckittas@uth.gr
[3] CREST- UMR CNRS 6000, Université de Franche-Comté, 2, Avenue Jean Moulin, 90000 Belfort, France; e-mail: roy@ige.univ-fcomte.fr
[4] Department of Biological Systems Engineering, Washington State University, 213 L. J. Smith Hall, Pullman, WA 99164-6120, USA; e-mail: shaojin_wang@wsu.edu

(Received 7 March 2001; accepted 12 July 2002)

In this paper, the characterisation and modelling of the most relevant convective transfers contributing to the description of the distributed greenhouse climate are studied in detail. After a brief review of the equations governing flows within the greenhouse, the major theoretical approaches are recalled. The focus is on the study of the distributed climate which requires the equations governing the fluid flow and includes the turbulent transfer. The digitisation of these equations and their solution using computer fluid dynamics (CFD) software are presented. The measurement techniques associated with this approach are also presented, with special attention paid to the determination of air flows and climate patterns using advanced flow measurement techniques such as particle imagery visualisation (PIV) and sonic anemometry. A complete panorama of the studies pertaining to air movement inside the various greenhouse types is presented and it is particularly focused on recent studies dealing with plant–air interactions, particularly the leaf boundary layer climate and the air flows within the crop canopy. Despite the difficulties of modelling turbulent transfers, it is shown that simulations involving CFD software are becoming more realistic and able to describe with good accuracy the main features of the distributed climate inside the greenhouse. The major consequences of this progress are discussed with respect to improvement of the greenhouse climate through better plant protection and enhancements of greenhouse design and control.

1. Introduction

It was shown in a companion paper (Roy *et al.*, 2002) that simple analytical solutions describing the convective exchanges combined with semi-empirical ventilation models were often sufficient in solving most classical engineering problems related to describing the greenhouse climate. Yet, the recent concerns on crop quality and preservation of the environment increasingly require that account should also be taken of climate heterogeneity and crop activity. Examples of cases where this is necessary are the optimisation of the vertical distribution of crop temperature and transpiration by means of low-temperature heating pipes localised in the crop rows (Kempes & van den Braak, 2000), the study of nitrate loses in lettuce grown in plastic tunnels in Mediterranean regions (de Tourdonnet *et al.*, 2001; Boulard & Wang, 2002), and the determination of the climatic dependence of bio-aggressors and antagonists involved in integrated pest management (IPM) strategies (Jewet & Jarvis, 2001; Boulard *et al.*, 2002). These problems cannot be solved using approaches based on the homogeneity of the greenhouse air because no details are provided on the inside climate patterns nor on the heterogeneity of crops or pest activity. Recent progresses in flow models using computational fluid dynamics (CFD) facilitate the analysis of this climate heterogeneity by solving transport equations in closed (Nara, 1979; Lamrani *et al.*, 2001) and ventilated greenhouses (Mistriotis *et al.*, 1997a, 1997b). This numerical approach requires further empirical validation, particularly in the case of the

Notation

a_1, a_2	regression coefficients
c	specific humidity of air, kg kg^{-1}
C_f	inertial factor of a porous medium
C_v	drag coefficient for the vegetation
C_μ	empirical constant for the closure of the turbulence model
d_v	water vapour diffusivity, m^2 s^{-1}
$\mathbf{f}$	resultant vector of the external acceleration applied on a fluid domain
$\mathbf{g}$	gravity vector
$\mathbf{J}_\Phi$	flux vector of the physical variable Φ in a fluid flow
K	permeability of a porous medium, m^2
l_l	leaf area index
P, ΔP	Pressure, pressure drop, Pa
Ra	Rayleigh number
Re	Reynolds number
Re$_p$	modified Reynolds number
S_Φ	sink or source term for the physical variable Φ
t	time, s
T, ΔT	Temperature, temperature difference, K
u	air speed, m s^{-1}
$\mathbf{u}$	velocity vector
u_i, u_j	components of the velocity vector, m s^{-1}
u_j'	fluctuation of the components of the velocity vector, m s^{-1}
x	length, m
α	thermal diffusivity of air, m^2 s^{-1}
ε	viscous dissipation rate of turbulent energy, m^2 s^{-3}
Φ	Physical variable transported in a fluid flow
$\bar{\Phi}$, Φ'	mean and turbulent physical variable transported in a fluid flow
κ	turbulent kinetic energy, m^2 s^{-2}
μ	dynamic viscosity of fluid, kg m^{-1} s^{-1}
ν	kinematic viscosity of fluid, m^2 s^{-1}
ν_t	turbulent viscosity, m^2 s^{-1}
ρ	fluid density, kg m^{-3}
τ	stress tensor applied on a fluid domain
Subscripts	
0	reference

turbulent regime that prevails in greenhouse conditions. Turbulent air flow and the sensible heat exchange associated with it have been measured in naturally ventilated large-scale multi-span greenhouses with the help of ultrasonic anemometers (Wang, 1998; Boulard *et al.*, 2000; Haxaire *et al.*, 2000). Laboratory experiments using laser Doppler velocimetry (Lamrani, 1997) or direct visualisation techniques by laser tomography (Roy *et al.*, 2000a, 2000b) have also been used to map steady-state flow fields with well-defined boundary conditions. A good correspondence between experimental and calculated features is generally found. These results highlight the origin of convective motions and air renewal together with the important spatial heterogeneity of the scalar and vector fields. It has already been demonstrated that the CFD approach may provide realistic simulations for a wide range of geometrical and boundary conditions and thus can help engineers and greenhouse manufacturers to improve greenhouse control and design.

This review takes into account all convective transfers involved in greenhouses. In the first section, the theory and basic equations governing flow motions are presented. In the second, a presentation of the experimental and modelling techniques of convective transfers is provided based on the heterogeneity of the inside air. The numerical and measurement procedures necessary in determining distributed climate are outlined and the question examined whether CFD simulations can describe with a good accuracy the main features of the distributed climate inside the greenhouse.

2. Theory

2.1. *Fluid flow equations*

2.1.1. *Governing equations*

An accurate description of a fluid flow in a three-dimensional domain is made by determining the velocity and pressure fields and other variable quantities like enthalpy, concentration of chemical species, *etc.*, which can be transported by the flow in the entire domain. The phenomenological model that links these variables is deduced from the conservation equation of each variable Φ in any fluid domain. Fluid is considered to be a continuous medium

$$\frac{\partial \Phi}{\partial t} = -\mathrm{div}\,\mathbf{J}_\Phi + S_\Phi \tag{1}$$

where: $\mathbf{J}_\Phi$ is the flux vector of Φ through the domain boundaries, S_Φ the production of Φ in the domain and t the time.

When Φ represents the mass of fluid flowing through the domain, the conservation Eqn (1) becomes the well-known *equation of continuity*:

$$\frac{\partial \rho}{\partial t} = -\mathrm{div}(\rho \mathbf{u}) \tag{2}$$

where ρ is the fluid density and $\mathbf{u}$ the flow velocity vector.

A second equation is obtained by substituting the momentum for variable Φ. The conservation Eqn (1)

then becomes the *Newton's second law of motion*

$$\frac{\partial(\rho\mathbf{u})}{\partial t} = -\text{grad}\, P - \text{div}(\rho\mathbf{u}\times\mathbf{u}) - \text{div}\,\tau + \rho\mathbf{f} \qquad (3)$$

where: P is the pressure, τ the stress tensor, $\mathbf{f}$ the resultant vector of the external acceleration applied to the fluid and $\times$ the tensor product operator.

2.1.2. *Simplifying equations*

All the quantities presented in Eqns (1) and (2) are time and space dependent. Nevertheless, for fluid flow problems relevant to ventilation characterised by low velocity fields and low gradients of transported quantities, physical properties are assumed to be constant. A second simplification concerns the dynamic behaviour of the fluid: a linear relation between stress and deformation is assumed (*Newtonian fluid*) including the dynamic viscosity μ, and consequently the fluid flow equations become (Bird *et al.*, 1965)

$$\text{div}\,\mathbf{u} = 0 \qquad (4)$$

and

$$\rho\frac{\mathrm{D}\mathbf{u}}{\mathrm{D}t} = -\text{grad}\, P + \mu\nabla^2\mathbf{u} + \rho\mathbf{f} \qquad (5)$$

where $\mathrm{D}\mathbf{u}/\mathrm{D}t$ is the substantive time derivative or 'material derivative' of $\mathbf{u}$ and ∇^2 is the Laplace operator. This equation is a simplified form of the *Navier–Stokes equation* for viscous fluids. Most flow fields can be described with Cartesian co-ordinates system. In those cases, x_i is the length according to the ith component of space, Eqns (4) and (5) become:

$$\sum_{j=1}^{3}\frac{\partial u_j}{\partial x_j} = 0 \qquad (6)$$

$$\rho\left(\frac{\partial u_i}{\partial t} + \sum_{j=1}^{3} u_j\frac{\partial u_i}{\partial x_j}\right) = -\frac{\partial P}{\partial x_i} + \mu\left(\sum_{j=1}^{3}\frac{\partial^2 u_i}{\partial x_j^2}\right) + \rho f_i \qquad (7)$$

where Eqn (7) is the ith component of the momentum equation.

For convective and ventilation situations, determination of the temperature and humidity fields is essential for understanding the climate in greenhouses. Assuming that the heat production due to molecular friction (viscous dissipation) is negligible, the conservation equation for temperature fields becomes

$$\frac{\mathrm{D}T}{\mathrm{D}t} = \alpha\nabla^2 T \qquad (8)$$

where T is the temperature and α the thermal diffusivity of air. The conservation equation for water vapour field becomes

$$\frac{\mathrm{D}c}{\mathrm{D}t} = d_v\nabla^2 c \qquad (9)$$

where c is the specific humidity of air and d_v the water vapour diffusivity. All the above physical properties are considered to be constant.

2.1.3. *Combining equations*

The dependence of the thermal field on flow velocity distribution is clearly demonstrated in Eqn (8). Conversely, the opposite combination does not appear to be explicit in Eqns (5) and (7). If this combination occurs, it takes place in the variation of the physical properties of fluids caused by temperature heterogeneity. For flow configurations like greenhouse flow patterns, the resultant $\rho\mathbf{f}$ of external forces is limited to the gravitational forces $\rho\mathbf{g}$ so that the influence of free convection caused by temperature gradients is evident. When buoyancy forces occur in the flow, the assumption of fixed physical properties no longer matches fluid flow behaviour. Free convection effects are taken into account in the momentum equation by the variation in fluid density due to a heterogeneous temperature field. If T_0 and ρ_0 represent reference values for temperature and density, the equation of state for density ρ becomes, using Taylor's development (Bejan, 1984)

$$\rho = \rho_0\left(1 - \frac{T - T_0}{T_0} + \cdots\right) \qquad (10)$$

The temperature dependence of density in Eqn (7) introduces a problem in solving this equation. The *Boussinesq approximation* is widely used to simplify the momentum equation: density is considered as constant $\rho = \rho_0$ for inertial terms, whereas Eqn (10) is used to quantify the leading body force term. This approximation can also be applied to other quantities influencing density, such as pressure, but the influence of temperature is predominant for free convection problems (Gray & Giorgini, 1976).

2.1.4. *Turbulence models*

The presence of turbulence in a fluid flow is indicated by fluctuations of velocity components and quantities transported by the flow, even when the boundary conditions for the problem studied are kept constant. These random fluctuations constitute the phenomenological difference with laminar flows which are deterministic. For most ventilation situations, experimental measurements and visualisations show the turbulent character of the inner and outer greenhouse flows. Consequently, turbulence phenomena must be taken into account in the fluid flow equations, in order to accurately quantify the transferred quantities (heat and mass transfer rates are appreciably increased by turbulence). Turbulence theory is too complex to be described here (Bradshaw, 1971; Tennekes & Lumley, 1972; Favre *et al.*, 1976), however, it is necessary to give

a description of the most frequently used models because they require the use of other conservation equations for fluid flow (closure equations).

The most common method for obtaining closure equations for turbulent quantities is to express each variable Φ as the sum of two parts: a mean quantity $\bar{\Phi}$ and a fluctuating one Φ'. This principle is applied both to velocity components and scalar quantities, and the fluid flow equations are time averaged. Consequently, new quantities like cross-correlations of variables (specially the cross-correlations of velocity components that constitute the *Reynolds shear stress*) appear in the equations. In the most widely used closure model, the so called 'κ–ε model', two new variables may be deduced from these fluctuations:

(a) *the turbulent kinetic energy* κ

$$\kappa = \frac{1}{2}\sum_{j=1}^{3}\overline{\left(u_j'\right)^2} \tag{11}$$

where u_j' is the fluctuation of the component u_j

(b) *the viscous dissipation rate of turbulent energy* ε

$$\varepsilon = \nu\sum_{j=1}^{3}\overline{\left(\text{grad}\, u_j'\right)^2} \tag{12}$$

where ν is the kinematic viscosity of fluid.

In the conservation equations for κ and ε, the turbulent kinematic viscosity ν_t appears, although it is not an intrinsic physical property of fluids, but depends on flow conditions. This term is determined with the help of the *Prandtl–Kolmogorov* assumption and leads to

$$\nu_t = C_\mu\frac{\kappa^2}{\varepsilon} \tag{13}$$

The coefficient C_μ and other empirical constants that appear in the conservation equations for κ and ε are determined from experimental results. The determination of these empirical constants proves the non-universal character of the κ–ε model of turbulence and its inappropriateness in predicting original configurations: the knowledge of flow conditions for relevant situations, such as jet plane, or flow on a solid wall is an essential condition for using correct empirical constants or functions.

Three major turbulence models which help determine more accurately turbulent quantities near solid boundaries have been developed.

(1) In the fully turbulent κ–ε model (Harlow & Nakayama, 1967; Launder & Spalding, 1972) all the grid points used for the discretisation of flow equations in the area of interest are considered in the fully turbulent region. Wall functions are used to determine turbulent quantities on solid walls.

(2) In the low Reynolds number κ–ε model (Launder & Spalding, 1972; Lam & Bremhorst, 1981), the grid is more refined in non-fully turbulent regions specially near solid walls where a damping function is taken into account as for example in Eqn (13) for determining the turbulent viscosity. Consequently, there is no need for wall functions.

(3) In the two-scale models (Chen & Kim, 1987) (CK) and in the renormalisation group (RNG) model (Yakhot & Orszag, 1986), two time scales are used for determining the turbulent kinetic energy κ.

The configuration of the area of interest and the influence on the flow field of the parts of the domain with a small size constitute the principal criteria for choosing the turbulence model. For example, the presence of small slot-vents in a laboratory leads to the use of the low Reynolds number κ–ε model (Hoff *et al.*, 1992). For greenhouse flow conditions characterised by separating and reattaching flows, a comparative study undertaken by Mistriotis *et al.* (1997b) has demonstrated that a two-scale model corresponds better with experimental data.

2.1.5. *Solving equations*

Owing to the non-linear character of the momentum equation, the analytical determination of the solutions of the system Eqns (6) and (7) is not possible, except for rare situations in one or two-dimensional flows where significant simplifications of the equations are possible (Schlichting, 1955). For greenhouse flow patterns characterised by three-dimensional conditions, it is impossible to obtain an analytical solution for velocity, pressure and others transported quantity fields. Nevertheless the different methods shown in *Fig. 1* have been developed in order to determine the climate and the heat and mass transfers in buildings and greenhouses. Behavioural models, such as neural networks (Seginer *et al.*, 1994; Krauss *et al.*, 1997) are very useful for establishing a control strategy, but they still depend on accurately determining flow-parameter values. These models must then be compared with experimental results or with a phenomenological model. The rapid development of numerical computational methods nowadays helps in obtaining approximate solutions of the phenomenological micro-model. These methods (called CFD methods) use a fine discretisation of the domain studied and will be presented in a later section concerning numerical computational methods of fluid flows.

2.2. *Convection in porous media*

The modelling of transported quantities in a flow (for example momentum, heat and vapour in a greenhouse)

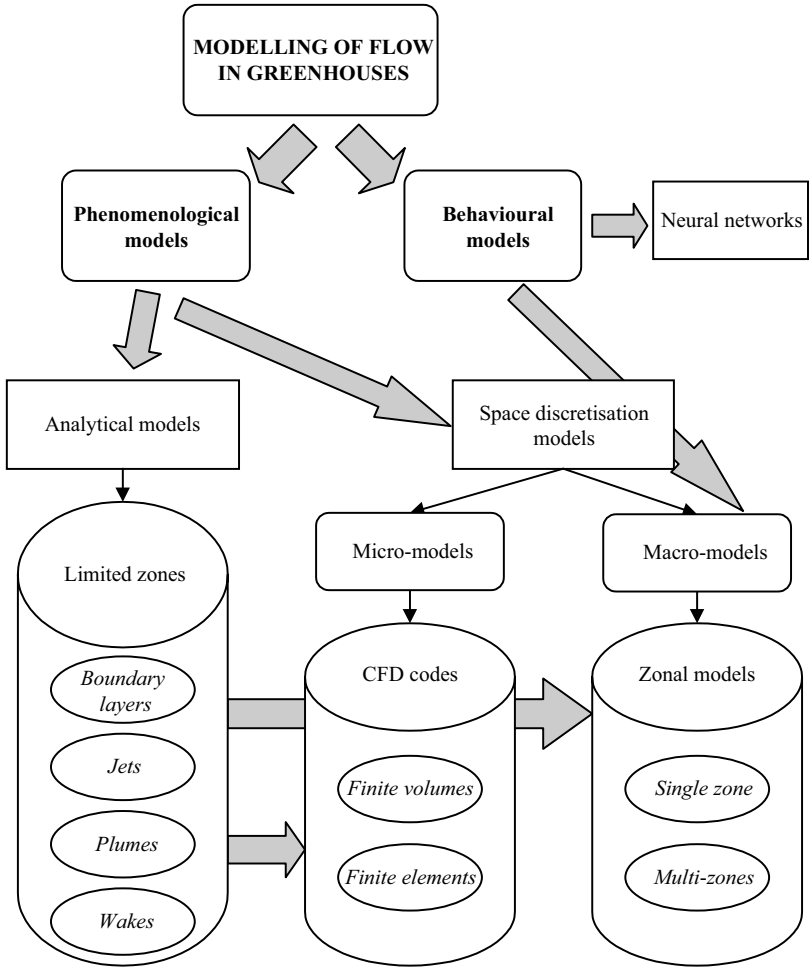

Fig. 1. Classification diagram of the simulation models; CFD, computer fluid dynamics (adapted from Krauss et al., 1997)

is essential for the understanding and the prediction of the crop response to external physical influences. However, it would be unrealistic to attempt to take into account transfers on each leaf for understanding and predicting the crop response. The definition and design of the three-dimensional domain of interest (leaves as solid bodies and air as fluid) is very complex: a solution to this modelling problem lies into considering the crop vegetation as a porous medium.

A porous medium can be defined as a solid matrix with interconnected pores through which the fluid flows. A structural property of this kind of medium is porosity, which is expressed as the ratio of the volume of the pores to the total volume (Nield & Bejan, 1992). The presence of a solid matrix in the flow leads to a considerable increase in the transfer of transported quantities like the momentum balance which is affected by the friction on the solid matrix. Flow modelling in a porous medium for a fluid-saturated control volume of that medium lies in the definition of its volume-averaged velocity vector (seepage velocity). The simplest model expressing the link between the pressure gradient and the velocity vector in the control volume is the *Darcy law*

$$\text{grad } P = -\frac{\mu}{K}\mathbf{u} \tag{14}$$

where the medium permeability K is independent of the nature of the fluid and depends only on the geometry of the pores in the medium. The Darcy law stands for the momentum equation Eqn (3) and its limitation is the absence of the inertial term u^2. The domain of validity of the Darcy law is defined by the modified Reynolds number Re_P

$$\text{Re}_p = \frac{uK^{0.5}}{v} \tag{15}$$

where u is the wind speed. The Darcy law is valid as long as $\text{Re}_P < 1$, i.e. when inertial terms have a smaller magnitude than viscous terms (Bejan, 1984). When Re_P is greater than unity, the quadratic term is taken into account using an extension of the Darcy law, the

Darcy-Forchheimer equation

$$\text{grad}\, P = -\frac{\mu}{K}\mathbf{u} - C_f K^{-0.5}\rho u\mathbf{u} \qquad (16)$$

where ρ is the fluid density and C_f a dimensionless inertial factor. This term is not constant and varies with the porosity of the medium. For greenhouse situations, where the permeability K of the crop is significant, the viscous term (the first term on the right-hand side of Eqn (16)) is negligible (the order of magnitude of the dynamic viscosity μ is 10^{-5} for air), so the pressure gradient only depends on the quadratic term alone

$$\text{grad}\, P \approx -C_f K^{-0.5}\rho u\mathbf{u} \qquad (17)$$

Consequently, factor C_f can be determined by measuring the pressure loss through a crop with different seepage velocity values (see Section 3.1.6).

3. Distributed climate

The greenhouse cover profoundly modifies the internal climate conditions compared to those outside. Generally, air velocity and radiation decrease, whereas temperature and air humidity rise and the CO_2 content fluctuates considerably. These conclusions are based on climatic measurements made at a representative fixed height, generally in the centre of the greenhouse. The difference is far more significant if we take into account a distributed climate and changes in crop activity. However, the presence of independently controllable regulation systems for local climate (pipe heating, ventilators, local humidification, CO_2 distribution and drip irrigation) may also locally influence crop growth and development (Kempes & van de Braak, 2000). The knowledge of the distributed climate at crop level should help to improve its homogeneity by modifying the design of the greenhouse structure and climate air conditioning systems and by locally controlling these systems. This requires the characterisation and modelling of the processes, particularly of convective transfers, involved in its elaboration.

3.1. *Characterisation*

3.1.1. *Techniques*

Although the interest in distributed climates in greenhouses dates from the beginning of the greenhouse industry (Carpenter & Bark, 1967), the first attempts to measure air circulation patterns in greenhouses were based on smoke generators showing differences in air movement in diverse locations. These results were merely qualitative and did not allow any comparison between experimental and simulated results. The first quantitative values of air flow patterns were obtained from dynamic pressure measurements performed in model scale greenhouses with steady state and well-defined boundary conditions (Nara, 1979; Sase *et al.*, 1984). In such conditions, even simple measurements can provide useful hints on flow and temperature patterns. Laboratory experiments performed in model scale greenhouses were also used later. These were often combined with laser Doppler anemometry (LDA) to map the flow fields in closed greenhouses (Lamrani *et al.*, 2001) or coupled with particle image velocimetry (PIV) (*Fig. 2*) to map the flow patterns in ventilated (Okushima *et al.*, 1998; Montero *et al.*, 2001a) and heated greenhouses (Roy *et al.*, 2000a, 2000b). A different method using a scale model of a greenhouse immersed in a water tank containing a salty water solution to produce density differences was used by Oca *et al.* (1998) and Montero *et al.* (2001b) to simulate buoyancy-forces-driven ventilation. For a laminar regime, flow is visualised with the help of a video camera and the method is used to test different ventilation arrangements for mono-span greenhouses.

Air and heat exchanges were first estimated in a bi-span greenhouse with a continuous vent using a one-dimensional sonic anemometer and fine thermocouples

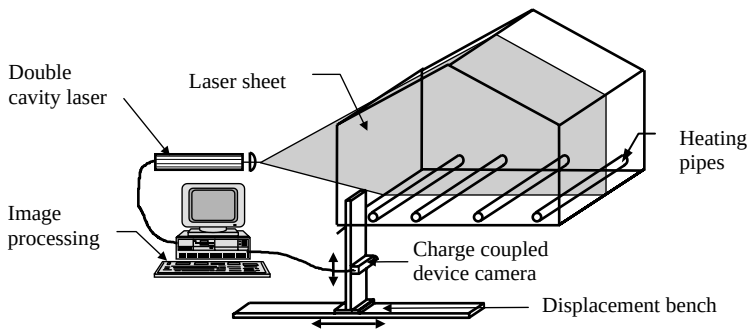

Fig. 2. Experimental arrangement for PIV measurements in a half-scale greenhouse (after Roy et al., 2000b)

(Boulard *et al.*, 1997). Further knowledge about the turbulent airflow and the associated sensible heat exchange were provided by measurements with a three-dimensional sonic anemometer operated in the whole greenhouse volume of the same bi-span greenhouse (Haxaire, 1999). Ventilation-induced air movement in a large multi-span greenhouse was later measured by means of a customised multi-point two-dimensional sonic anemometer (Wang & Deltour, 1999; Wang *et al.*, 1999). Moderate-speed airflow measurements were also performed in a tunnel greenhouse to map air movements and microclimatic heterogeneity and to evaluate the turbulent characteristics of air velocity components (Boulard *et al.*, 2000). With only one or two sampling positions for sonic anemometers at any one time, the changing external conditions during the time needed to explore the whole greenhouse volume posed a problem. This problem was overcome by selecting measurements for the prevailing external wind direction and by using the external wind speed and the difference in air temperature and humidity between the inside and the outside as scaling parameters.

Air temperature measurement techniques have not changed much since air temperature patterns were first determined (Carpenter & Bark, 1967; Nara, 1979) until now (Lamrani *et al.*, 2001). Greenhouse air and surface temperatures were measured by means of very small thermocouples placed on a grid with a variable mesh. Recently, the three-dimensional sonic anemometer makes it possible to directly measure air temperature as well as the three-dimensional components of air speed (Boulard *et al.*, 2000).

3.1.2. *Airflow patterns and associated flux in closed greenhouses*

In closed greenhouses, buoyancy forces mainly drive convection whereas in ventilated greenhouses wind forces prevail, alone or in combination with buoyancy forces. Nara (1979) first studied the temperature patterns in a 1/2 scale mono-span greenhouse with a moderate temperature difference between a heated floor simulating the absorption of solar radiation and a colder roof. In steady-state conditions with laminar regime, the measurements indicated two symmetrical rotations of airflow for an approximately square span (height–width). But a single loop occupying the whole volume was evidenced with non-symmetrical soil temperature boundary conditions (imposed heat flux). In both cases, a temperature inversion (rise of temperature with the height), speeded up by an increase of the Rayleigh number Ra was noted. Lamrani (1997) has used LDA to characterise flow patterns under similar experimental conditions, but with an imposed flux instead of temperature at soil level. For turbulent conditions

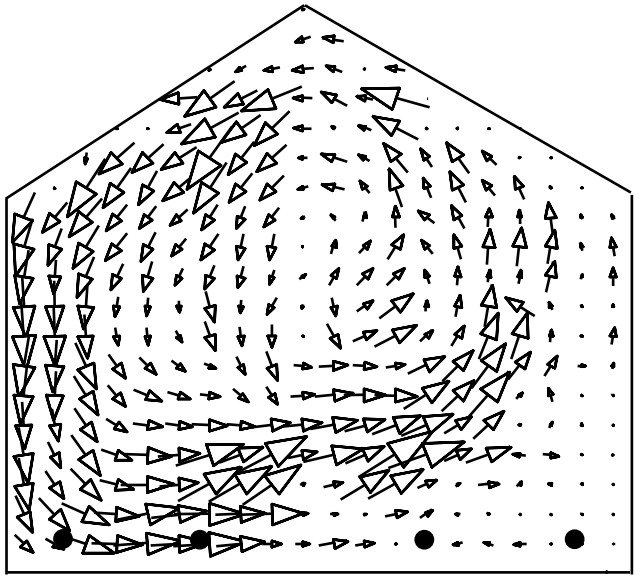

Fig. 3. Flow pattern in a closed heated half-scale greenhouse determined with PIV technique; ●, heating pipe (after Roy et al., 2000b)

(Ra $\sim 10^9$ and 10^{10}) corresponding to the flow conditions commonly found in full-scale greenhouses, he always found a single loop occupying the whole span, with high speed along the floor walls and the roof and still conditions in the core of the greenhouse. The air temperature decreased mainly in the first 5 cm over the heating floor, but remained almost unchanged over the whole cavity volume, before decreasing again in the 25 cm immediately below the roof surface. Experimental air–soil and air–roof convective transfer formulas were deduced from these studies and a vertical profile of the turbulent flow components was also presented.

Flow patterns induced by pipe heating in the same 1/2 model scale mono-span greenhouse were later studied by Roy *et al.* (2000b) using PIV. Surprisingly, the natural convective patterns observed (*Fig. 3*) were similar to those due to the absorption of solar energy at floor level (Boulard *et al.*, 1997). Compared to the classical approach applied to a homogeneous greenhouse volume, these experiments indicate the existence of a vertical heterogeneity of the scalar and vector fields due to a single loop that occupies the whole space of each span and develops vertically between warm (soil, pipes) and cold (roof) surfaces.

3.1.3. *Air flow patterns and associated flux in open greenhouses*

Buoyancy flow in a mono-span greenhouse. The 1/2 model scale mono-span greenhouse already used to characterise air movements in closed greenhouses (Lamrani, 1997) was later equipped with vents on both

roof slopes and employed to study buoyancy-driven ventilation (Boulard *et al.*, 1998). The flow patterns in two-dimensional vertical cross-sections always exhibited a single convective loop for single- and two-sided ventilation with soil heating as well as with pipe heating. This flow pattern is similar to the one observed in closed greenhouses. With only one roof vent (*Fig. 4*), the convective loop is fed with cold air coming in through the lower part of the vent, flowing along the walls, the floor and the roof of the cavity before flowing out through the upper part of the vent opening. A single convective loop fed with cold air entering the lower parts of the two vents and flowing out from their upper parts had also been observed for two-sided symmetrical ventilation. As in closed greenhouses, this loop can rotate either clock-wise or anticlock-wise depending on the initial boundary conditions.

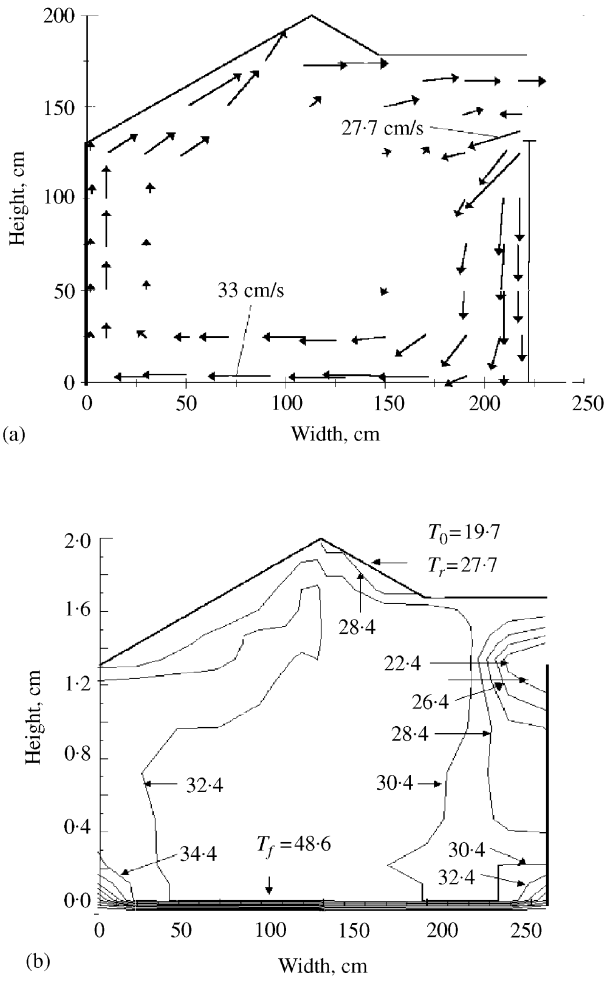

Fig. 4. (a) Velocity field and (b) temperature °C field measured in a half-scale floor-heated greenhouse with a continuous roof-vent; T_0, reference temperature; T_r, roof temperature; T_f, floor temperature (after Boulard et al., 1999)

In both cases, the thermal boundary layer only extended over a short distance (5–6 cm), whereas velocity gradients extended much further, 50 cm away. Consequently, vertical temperature profiles are characterised by a strong gradient situated just above the floor. Detailed photography of the flow in the vents with the help of laser tomography has also shown that the inflow speed was greater than the outflow speed, but affected a smaller section.

Ventilation rate values deduced from measurements by means of a sensible heat balance in the model scale greenhouse were in agreement with values obtained by the application of Bernoulli's theorem with a simple discharge coefficient. But flow measurements in greenhouses with two-sided openings did not have twice the ventilation rate of greenhouses with one-sided opening as predicted by Bernoulli's theorem.

Wind effect in a mono-span greenhouse. Sase *et al.* (1984) studied the combination of wind and stack effects in a 1/10 scale single span greenhouse equipped with continuous side and ridge ventilators. The predominant wind effect ($u > 1$–$2\,m\,s^{-1}$) was primarily affected by the configuration of the ventilator through which fresh air enters, whereas the stack effect was mainly affected by the combinations of ridge and side ventilators. Sase demonstrated considerably higher temperatures in the inner space adjacent to the windward gable end and lower temperatures in the inner space adjacent to the leeward gable end (*Fig. 5*) with wind approximately parallel to the gutters. This three-dimensional distribution of temperatures was corroborated later by other authors and suggests an inflow through the openings situated at the leeward side and an outflow through the openings situated near the windward gable end.

Wind effect in multi-span greenhouses. Airflow patterns induced by wind effects in a bi-span Venlo-type greenhouse were studied using particle imagery visualisation in wind tunnel experiments by Okushima *et al.* (1998). The results revealed very complex airflow patterns with significant exchanges through the windward and leeward ventilators, and with much less important exchanges through those other than windward and leeward vents.

The first attempts to determine *in situ* the flow and temperature distributions were made using mono-dimensional sonic anemometers placed in the vent opening in a full scale bi-span plastic-house (416 m^2) with continuous vents at the gutter level (Boulard *et al.*, 1996). The volume explored was later extended to the whole surface situated at the openings using three-dimensional sonic anemometry (Boulard *et al.*, 1997)

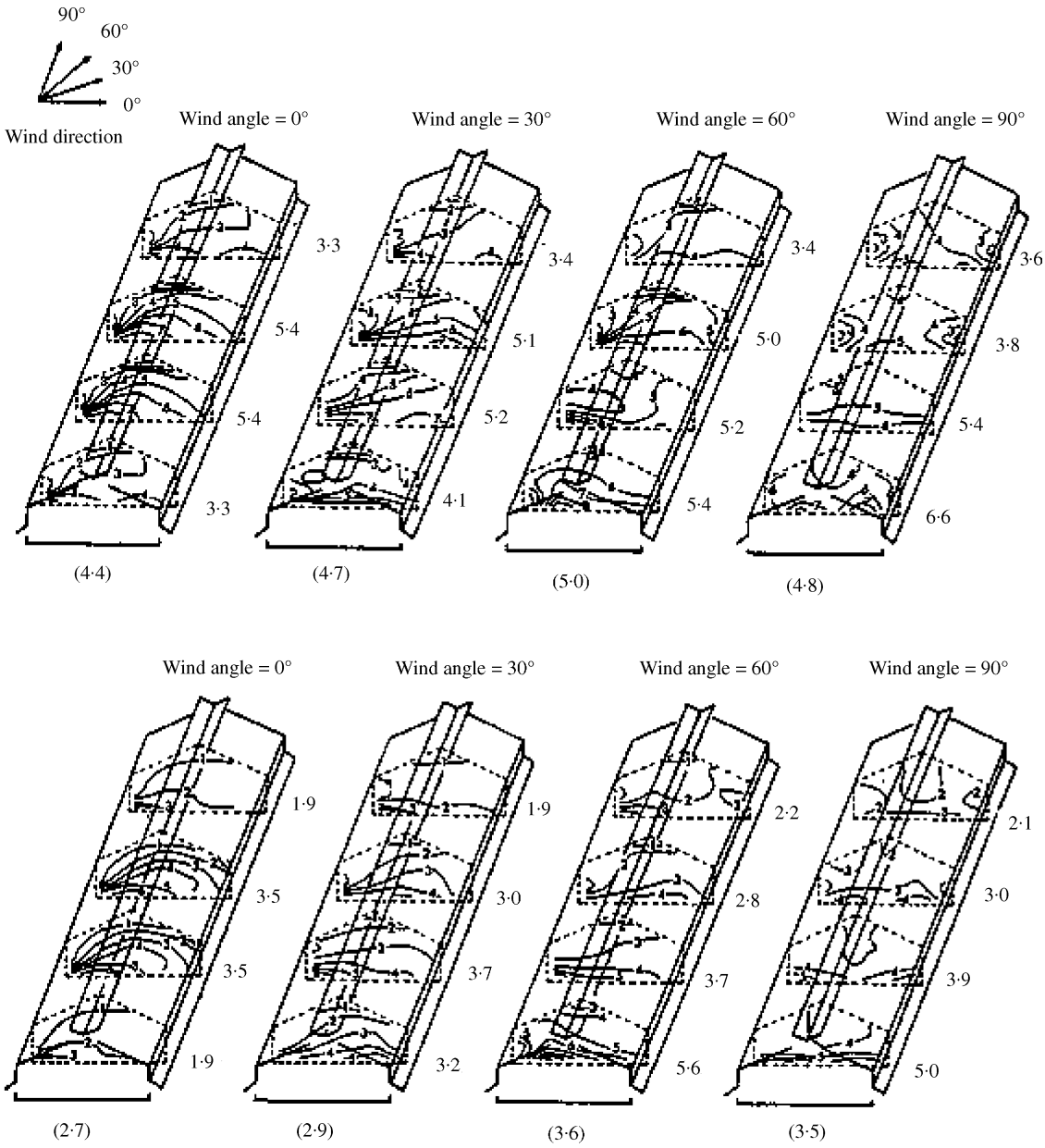

Fig. 5. Spatial distribution of temperature rise in °C with changing wind direction at reference wind velocities of 1·0 m s^{-1} (upper) and 4·6 m s^{-1} (lower) measured in wind tunnel testing of model scale 1/10 greenhouse. The value on the right of each transverse section and the value in parenthesis denote the average temperature in the crop space of the section and the average over four sections, respectively (after Sase et al., 1984)

and then, associated with humidity measurements, to the whole greenhouse volume (Haxaire, 1999). Both the turbulent and sensible heat exchanges were characterised with the contribution of the turbulent part representing between 23 and 45% of the exchanges. As already observed by Sase *et al.* (1984) on model-scale, a wind blowing parallel to the greenhouse ridge gave rise to an inflow on the downwind side and an outflow on the windward end. As shown in *Fig. 6*, cold and dry outside air penetrated into the greenhouse through the leeward part of the roof vent opening, flew in counter current with respect to wind direction in the volume occupied by the crop, before escaping through the first 2 m of the opening situated at the windward end. In the same greenhouse, Wang *et al.* (1999) have systematically measured the inside air speed at crop level and showed

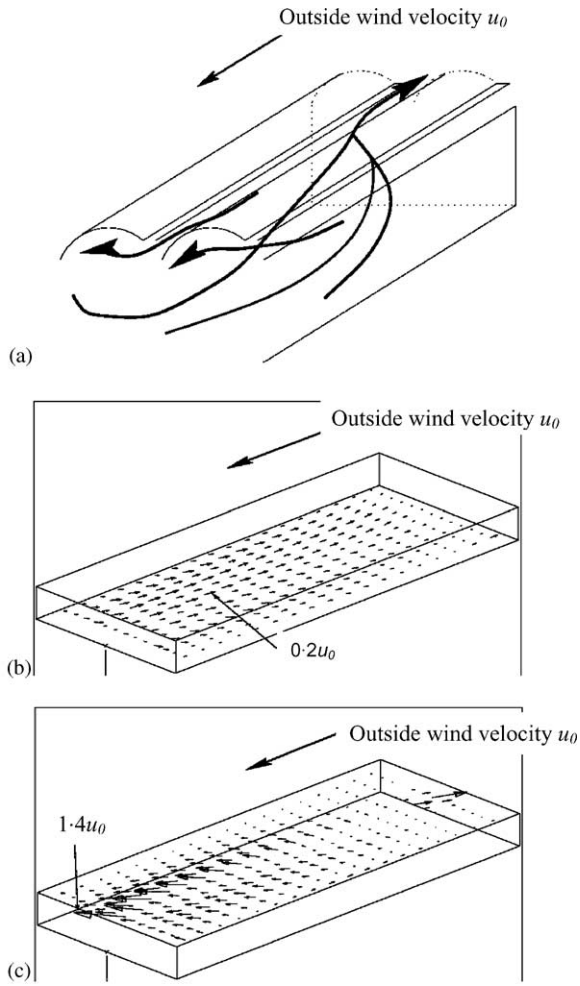

Fig. 6. Airflow patterns measured in a bi-span greenhouse equipped with continuous roof vent openings parallel to the wind direction for (a) general circulation of airflow; (b) horizontal air velocity field measured at the level of the crop cover (0·65 m); and (c) horizontal air velocity field measured at the level of the roof openings (3 m) (after Haxaire, 1999)

that it could be related to the external wind speed and the vent opening surface. A similar air circulation scheme characterised by a counter current flow with respect to wind direction was also characterised by Wang and Deltour (1999) in large-scale multi-span Venlo-type greenhouses.

Wind effect in tunnels. Measurements of the temperature fields inside small tunnels (0.6 m high) ventilated with the help of different perforation schemes demonstrated that a quincunx arrangement with alternatives holes at the top and the sides gave the best homogenisation of the thermal fields and air exchanges, especially in wind-less conditions (Baille, 1975).

For wind perpendicular to the axis of a 7 m tunnel with openings obtained by local separation of plastic sheets, Boulard *et al.* (2000) studied the mean and turbulent airflow along with patterns of air temperature and humidity transport. Measurements with three-dimensional sonic anemometers and fast response hygrometers revealed a strong current crossing the tunnel between the windward and leeward openings and moderate air velocities in the vertical section situated between two consecutive series of openings. The air temperature pattern was characterised by a temperature gradient due to cold air penetration through the vent opening and a vertical gradient above the soil surface due to solar energy absorption at soil level. Specific humidity patterns were different from air temperature patterns, with 'humid' areas concentrated only along the soil surface close to the source of evaporating water. Turbulence intensity increased from the centre of the tunnel to the windward opening, where it was about ten times greater than in the centre of the tunnel. Average air speeds ranged between 20 and 80% of outside wind speed, while it was only 10 and 20% in greenhouses equipped with roof openings.

3.1.4. *Interactions between airflow and crop cover*

The analogy with plate exchangers or finned tubes used in mechanical engineering problems has often been applied to study heat and mass transfers from plants. Local convective coefficients were derived from this approach (Parkhurst *et al.*, 1968; Cowan, 1972) and then used for determining the sensible and latent heat exchanges for numerous greenhouse crops such as tomato (Stanghellini, 1987), lettuce (Pollet & Bleyaert, 2000), cucumber (Bakker, 1986; Yang *et al.*, 1990), rose and ornamental plants (Baille *et al.*, 1994). However, because of the complexity of the system, data on actual greenhouse internal convection in the presence of a crop were scarce and the dynamic, energetic and mass exchange interactions between crops and airflows could hardly be analysed.

Dynamics Effect of greenhouse crops. Only rare experimental studies have been devoted to the effect of greenhouse crops on flows. The effect of tomato plant arrangement on airflow characteristics has been studied by Sase (1989), in a naturally ventilated greenhouse equipped with side and roof vents. He showed that the velocity coefficient (ratio of inside to outside air speed) was twice as great (0·4) when the wind was parallel to the row than when the wind was normal to the row direction (0·2). When only the ridge vents were open, the velocity coefficient was smaller (0·12) and depended neither on row direction nor on wind direction. In a greenhouse occupied by mature tomato crops and equipped with

roof vents, similar velocity coefficient values (between 0·1 and 0·15) were found by Wang *et al.* (1999).

In model-scale studies, Roy *et al.* (2000b) have shown that the presence of a tall crop such as a mature tomato crop does not change the flow pattern but reduces the turbulence of the flow, the crop playing the role of a porous medium generating a distributed pressure drop in the greenhouse volume (*Fig. 7*). These observations confirm previous studies on natural convection above heating pipes in greenhouse canopies (Aubinet & Deltour, 1994) relating the particular behaviour of the 'crop cell plume' to the presence of heat and momentum sinks in the cell crop.

Sources and sinks of heat and water vapour. Only scarce data, most of them on closed greenhouses, are available on the heat and water vapour exchanges between crops and greenhouse air. Aubinet and Deltour (1994) who studied natural convection above heating pipes in greenhouse tomato canopy and characterised the plume generated by the heating pipes in the crop rows. More recently, Kempes *et al.* (2000) have described the effect of heating system position on the vertical distribution of crop temperature and transpiration. In a closed greenhouse with mature pepper plants in diurnal conditions, Zhao *et al.* (2001) observed strong vertical air temperature and humidity gradients induced by the interception of solar radiation by plants. These gradients decrease as the greenhouse is cooled down when the roof windows are open. When both roof and side vents are open, the temperature and humidity gradients are larger than with only roof vents open, and they are always negligible with small plants.

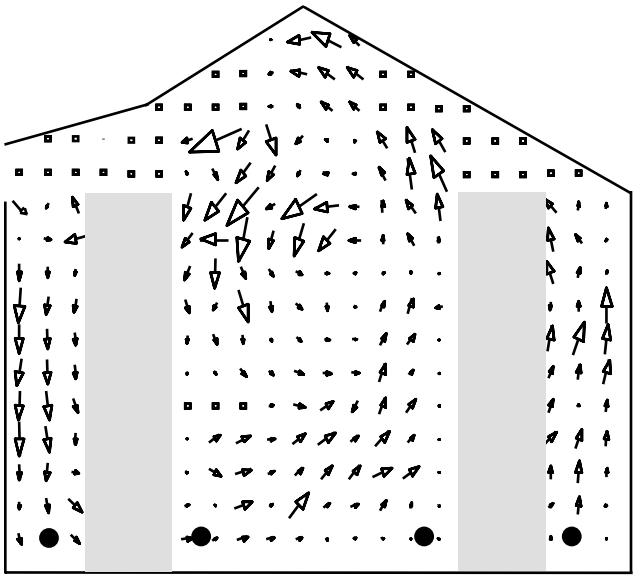

Fig. 7. Flow pattern in a opened heated half-scale greenhouse with tomato crop determined with PIV technique; ●, heating pipe; □, crop (after Roy et al., 2000b)

3.1.5. *Leaf boundary layer climate*

As insect pests are small in size and are to be found at the lower surface of the leaf (particularly whiteflies), Jewet and Jarvis (2001) suggested that the value of air humidity in this micro-climate may be increased owing to plant transpiration at the insect level. Schuepp (1993) reviewed studies on leaves both in free and forced convection and discussed particularly the implications for leaf morphology of the local microclimate. Velocity and temperature profile measurements were presented, but no examples of measured or modelled humidity profiles within the boundary layer were specified. More recently, Boulard *et al.* (2002) have studied the efficiency of the myco-insecticides for white-fly control in greenhouse situations with respect to the high-humidity requirements for infection and particularly to the humidity conditions prevailing in the boundary layer of the under leaf surface, i.e. in the habitat of the targeted white-fly larvae. Given the low air speeds observed in greenhouse conditions, the theoretical basis of the transfers within the leaf boundary layer for laminar conditions was presented and a model of air temperature and humidity distribution was proposed. Based on an experimental approach in full-scale greenhouse conditions, air humidity conditions within the under leaf boundary layer of a greenhouse tomato crop were investigated and an important increase in air humidity was detected at 5 mm beneath the under leaf surface. The increase in air humidity was particularly significant during day-time when crop transpiration was a maximum (*Fig. 8*). These measurements were compared with the results of the model based on the boundary layer theory and it was shown that the observed phenomena had been well predicted by the model, both qualitatively and quantitatively.

3.1.6. *Flows through nets and screens*

Nets and screening materials are often used in the greenhouse industry as windbreaks or as thermal and shade screens and to obstruct the movement of insects through opening. When air moves through a screen, it exerts a force on the screen so that the static pressure created across the screen reduces air flow.

These forces are to be measured in order to improve the design of screens and ventilation systems. Pearson and Owen (1992) and Kosmos *et al.* (1993) measured the pressure drop across these different components for air speeds between 0·05 and 1·7 $m\,s^{-1}$. They found that, despite the low Reynolds number of the air flow

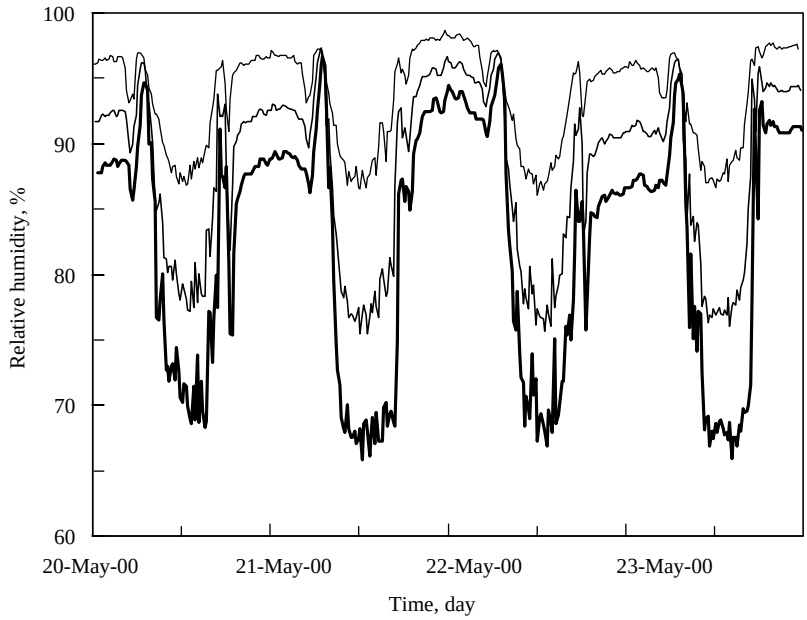

Fig. 8. Relative humidity of air, 1 mm (thin line), 5 mm (medium line) beneath the under leaf surface and in ambient air (thick line) (after Boulard et al., 2002)

($\mathrm{Re} \sim 100$), the pressure drop varies with the square of the air velocity according to Eqn (18).

In accordance with the Darcy–Forchheimer equation, Eqn (16), for lower air speeds ($0 < \mathrm{Re} < 100$), Miguel *et al.* (1998) consider both a quadratic term and a linear term with u which becomes significant for very low air speed

$$\Delta P = a_1 u^2 + a_2 u \tag{18}$$

where values for the coefficients a_1 and a_2 were determined by using regressions between experimental and theoretical values of pressure drops and air speed for various screens and nets.

A similar experiment was conducted by Miguel *et al.* (1997) using the Darcy–Forchheimer equation to express the airflow characteristics of currently employed greenhouse screens in terms of permeability K and inertial factor C_f.

Brundrett (1993) experimentally determined the correlation between the dynamic properties and the texture of the net and more particularly between its pressure loss coefficient and screen porosity. Experimental data from a wind tunnel were used by Teitel (2001), to compare different available methods to predict the pressure drop through screens. It is shown that comparing different screens by plotting their pressure drop *versus* the upstream velocity may be misleading. The weave texture is also important (Teitel & Shlykar, 1998) if the spacing between two adjacent threads of the screen is small in comparison with the thread diameter. The reduction of ventilation caused by the different kinds of screen (anti-thrip, anti-aphid and shade screens) was quantified by Montero *et al.* (1997) and Kittas *et al.* (2002) in multi-span arch-type greenhouses and discharge coefficient expressions were determined. In particular it was established that windows equipped with anti-thrip screens had a discharge coefficient approximately half of that of a window without a screen.

Fatnassi *et al.* (2001b) measured the climate in a very large Canarian-type greenhouse (6000 m^2) equipped with protection against whiteflies and estimated the ventilation rate using tracer gas measurements. The insect-proof net induced an additional pressure drop which reduced ventilation rate and significantly increased air temperature. They demonstrated an increasing reduction of ventilation rate induced by insect-proof net against whiteflies, anti-aphid nets and anti-thrip nets.

3.2. *Numerical computational methods of fluid flows*

3.2.1. *Natural convection by buoyancy forces*

Nara (1979) was one of the first researchers to perform numerical simulations of air circulation within greenhouses. He used the vorticity and stream functions as field variables to solve the finite difference scheme of the Navier–Stokes equation for a two-dimensional cross-section of a mono-span greenhouse with a fixed

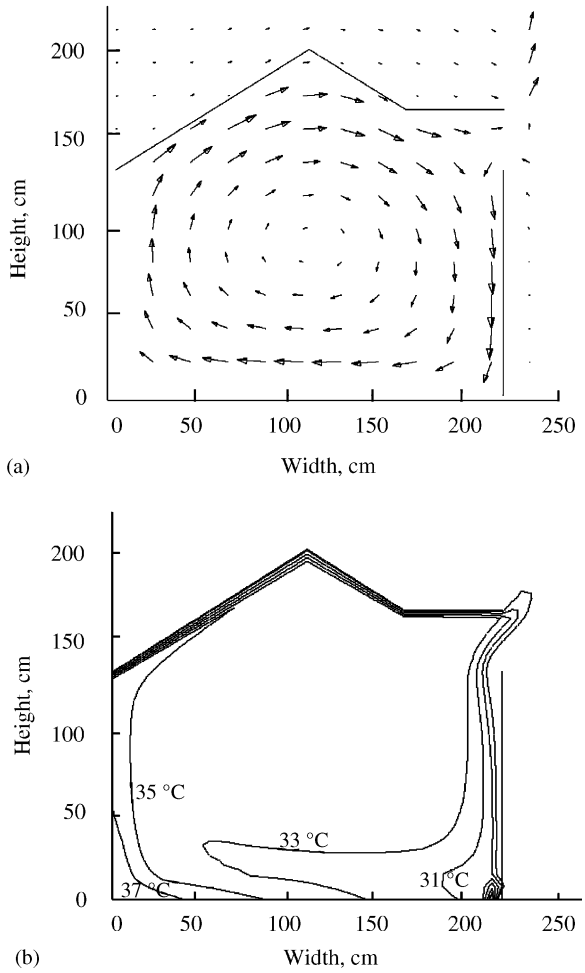

Fig. 9. (a) Velocity field and (b) temperature field simulated in a half-scale floor-heated greenhouse with a continuous roof-vent (after Boulard et al., 1999)

temperature difference between a warm soil and a colder roof to simulate soil surface heated by solar radiation. Simulations of free convection generated above the soil were performed for laminar conditions for Rayleigh numbers Ra ranging between 10^4 and 10^8 (the onset of transition to turbulence occurs for Rayleigh numbers between 10^6 and 10^{10}). In these conditions, primary rotations of airflow with two vortices were observed. However, under unsymmetrical temperature boundary conditions at roof or soil level as is often the case in full-scale greenhouses, only one primary vortex was generated.

The same geometric configuration was studied using CFD for larger Reynolds number values corresponding to Rayleigh numbers as high as 10^{13} (due to the large size of the greenhouses and the significant temperature differences) by Lamrani (1997) and Boulard *et al.* (1998). The standard version of CFD2000® was used to simulate the turbulent flows for approximately the same boundary conditions as Nara (but with an imposed flux instead of imposed temperatures at soil level) and with turbulent codes based on the standard κ–ε model (*Fig. 9*). The calculated and experimental results evidenced a single rotating air loop with high speeds along the floor roof and walls and still conditions in the core of the greenhouse. Experimental temperature and mean and turbulent flow patterns largely corresponded with calculated ones.

The same experimental device was later used to study steady-state temperature and flow patterns induced by ventilation with single-sided and two symmetrical roof vents (Boulard *et al.*, 1999). However, despite the good overall agreement between CFD simulations and measurements, a detailed comparison of the results has shown that the quality of the simulations could still be improved.

3.2.2. *Wind-driven ventilation*

Due to the importance of the turbulent effects in forced ventilation, turbulent flow models with high Reynolds number are required. Wind-induced flow and temperature patterns in a two-dimensional mono-span greenhouse equipped with roof and side walls vents were first simulated by Okushima *et al.* (1998) using a finite difference scheme with staggered grid and a two equations model (κ–ε). Validation with respect to wind tunnel measurements for side and roof hinged vents showed (Sase *et al.*, 1984) that the fit was good, except for an under-estimation of air velocity through the open windward vents attributed to a slight sensitiveness to sharp changes of air speed. When only two side ventilators are open, experiment and simulation showed patterns indicating an airflow passing through both side openings with a small recirculation eddy in the upper half-space of the greenhouse. Some discrepancies in these eddies may be attributed to the excessively coarse meshes in the regions where the reverse flow is observed. A three-dimensional analysis of the ventilation process was more recently performed by Mistriotis *et al.* (1997b) using commercial CFD software (Phoenics®) with various turbulence models (*Fig. 10*). Comparisons of simulations with experimental results obtained by Sase *et al.* (1984) have shown that the accuracy of the computational prediction was found to be satisfactory when a two-scale κ-ε turbulence model such as the CK or RNG models (see Section 2.1.4.) is used for describing the turbulent transport. These simulations were also validated against experimental data for bi-span greenhouses with the wind parallel to a continuous vent opening (Boulard *et al.*, 1996) and a good agreement between the numerical and experimental data was found when two-equations turbulence models were

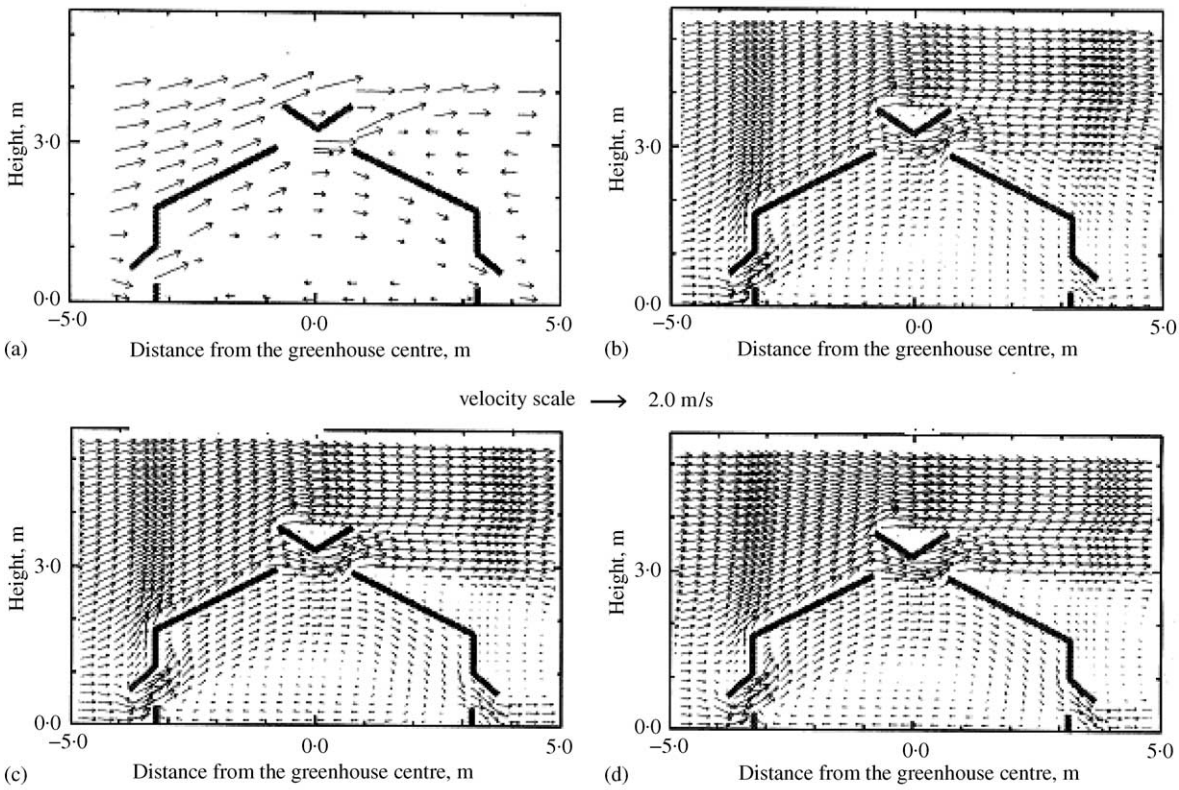

Fig. 10. Mean velocity vector field in a single span greenhouse obtained by various methods; (a) EXP—wind-tunnel experiment showing relative wind velocity vectors (after Sase et al., 1984); (b) CFD—κ–ε model showing absolute wind velocity vectors; (c) CFD—Chen—Kim (C–K) model showing absolute wind velocity vectors and; (d) CFD—renormalisation group (RNG) showing absolute wind velocity vectors. In all numerical simulations, the wind speed at 10 m high is 2 m s^{-1}; CFD, computational fluid dynamics (after Mistriotis et al., 1997b)

applied. The influence of design characteristics such as greenhouse length on ventilation was latter examined and the natural ventilation process was analysed at low-wind speed conditions (Mistriotis *et al.*, 1997b).

Using CFD software (Fluent®), Kacira *et al.* (1998) predicted two-dimensional airflow and temperature patterns in a multi-span saw-tooth greenhouse for various roof and side vents with windward or leeward (with respect to the vents) wind. Ventilation rates were also deduced and the respective efficiency of vents was analysed with respect to wind direction, vent designs and their combinations. The structural characteristics of naturally ventilated multi-span greenhouses were evaluated more systematically by Lee and Short (2000), who also studied the effect of the number of spans and of the presence of a hinged open roof.

Reichrath and Davies (2001) simulated a two-dimensional full-size commercial multi-span glasshouse comprising 60 spans with the help of Fluent®. A very large computational domain was chosen (450 m by 100 m) to minimise the influence of the boundaries and a logarithmic wind profile was defined at 50 m upstream of the glasshouse.

All the previous results were obtained without plants. Lee and Short (2000) later studied the dynamic influence of tall crops on airflow. Various wind directions and speeds, vent opening sizes and the presence of plants were studied for their influence on natural ventilation rates and airflow distributions. Air exchange rate was predicted to be strongly affected by the side vent opening size when it was windward. The average air exchange rate with plants was predicted to be 12% less than the rate without plants, but only 2·6% less for leeward side openings.

A three-dimensional study was performed and validated against experimental values of temperature and air speed in a leeward ventilated bi-span (400 m^2) plastic greenhouse occupied by a tomato crop (Haxaire, 1999; Haxaire *et al.*, 2000). The porous medium approach was used to model the dynamic effect of the crop on the flow and a standard κ–ε model assuming the isotropy of turbulence was adopted to model turbulence. This three

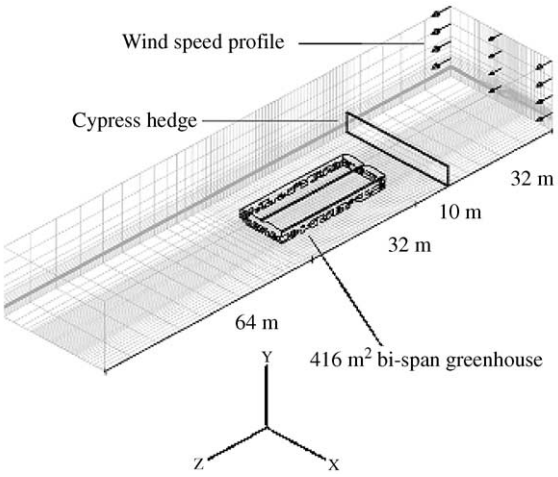

Fig. 11. Scheme of the studied domain and numerical grid for the CFD simulation of airflow and temperature patterns in a greenhouse with roof vent openings parallel to the wind direction. Boundary conditions: the two sides and the roof of the studied domain correspond to null-pressure-type conditions and the soil surface and the greenhouse walls are wall-type conditions; the cypress hedge is assimilated to a porous medium (after Haxaire, 1999)

dimensional simulation had considered a very large control volume (*Fig. 11*) with a length of 134 m, width 32 m and height 20 m, including the greenhouse itself (26 m long, 16 m wide) and a cypress windbreak situated at 10 m upwind. A wind profile calculated from experimental data was imposed as dynamic boundary conditions for ambient air. In accordance with measurements taken inside the greenhouse, simulations have confirmed that for pure leeward ventilation, outside air penetrated through the leeward side of the openings, flew counter current to outside wind in the space occupied by the crop before escaping through the windward part of the openings. It demonstrated that convection motion and air renewal is caused by wind pressure gradient developing along the entire length of the vent openings, particularly between the windward end (low pressure) and the leeward end (high pressure). As has been already observed in Section 3.1.3, similar flows corresponding to purely leeward ventilation already been characterised by Boulard *et al.* (1997) in a bi-span greenhouse and Wang and Deltour (1999) in a Venlo greenhouse with roof openings and by Lee and Short (2000) in a hinged open roof multi-span greenhouse. Mistriotis *et al.* (1997b) used the CFD simulations for a parametric study of the effect of the greenhouse length (32 m, 64 m, 96 m long) on the inside flow pattern. The behaviour of the 96 m greenhouse was different from the others as a second outflow occurred at the back of the greenhouse (there was an air-inlet in the middle of the greenhouse). Reichrath and Davies (2001) confirmed the occurrence of a reverse flow in the windward part of the greenhouse and of a dead zone with low velocity at approximately 60% of the total glasshouse length (*Fig. 11*) for a very large Venlo-type greenhouses (60 spans) under similar purely leeward ventilation conditions.

With boundary conditions measured in the experimental study, Fatnassi *et al.* (2001a) used CFD 2000® to simulate the three-dimensional air flux, temperature and humidity patterns in a large-scale greenhouse with side openings on both windward and leeward ends. In these conditions, the inside air flow is roughly parallel to the outside wind. In order to simulate also the pressure drop in the insect-proof net and to couple the flow with the cover, the CFD code was customised according to the method described in Section 3.2.3. Very complex flow patterns were observed, but good agreement was found between measured and calculated values of the ventilation rate. A similar study was performed in two dimensions with CFD 2000® by Bartzanas *et al.* (2001) for a smaller mono-span greenhouse equipped with insect-proof net against whiteflies on the side openings. The effect of different wind directions was also investigated, and it was shown that wind direction considerably affects the climatic conditions in the greenhouse when the greenhouse is equipped with insect screens.

3.2.3. *Combining the flow and the crop cover*

The flow and the crop cover exchange momentum, heat and mass. The interposition of a crop cover in an air flow gives rise to a fall in momentum and the absorption of solar energy by the leaves is accompanied by sensible heat, water vapour (transpiration) and CO_2 (photosynthesis) exchanges, so that all these aspects must be considered in conjunction with the use of CFD.

The sink of momentum. The sink of momentum due to the drag effect of the crop corresponds to the term $-\text{grad}\, P$ of the Navier–Stokes equation [Eqn (5)]. This drag force can be expressed by means of a commonly used formula (Thom, 1971) linking the drag effect to the leaf area index l_l and the air velocity $\mathbf{u}$, by means of a drag coefficient C_v:

$$\text{grad}\, P = L_l C_v \rho u \mathbf{u} \tag{19}$$

For a mature greenhouse tomato crop, Haxaire (1999) used wind tunnel facilities to calculate a value for C_v of 0·32. This value can be compared to a value for C_v of 0·30 calculated by Green (1992) to characterise a forest tree and to C_v of 0·20, proposed by Bruse (1995) for plant associations in general.

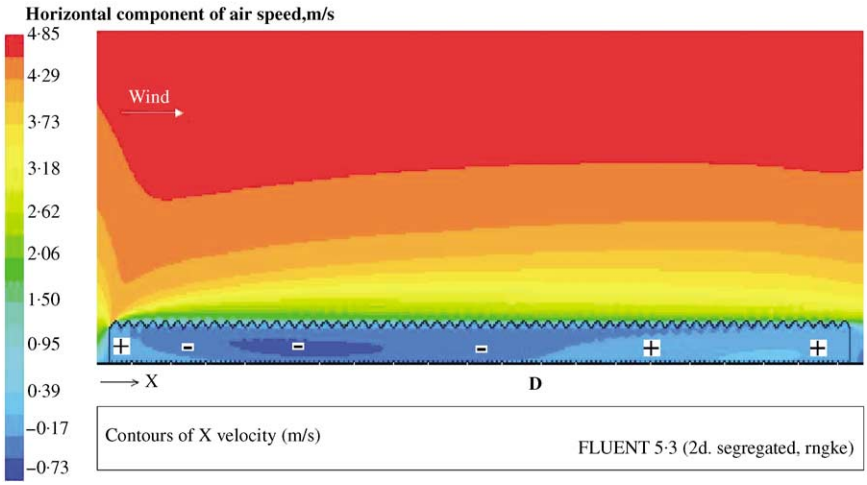

Fig. 12. Predicted X-velocity distribution in and around a 60 span Venlo-type glasshouse under leeward ventilation with a reference velocity at ridge height of 3·5 m s^{-1} and using a renormalisation group (RNG) turbulence model. The total spans are schematised along the X-axis and the signs + or – in the figure refer to the areas within the greenhouse space with a positive or negative X-velocity. The point D indicate the place where the flux is reversed (after Reichracht & Davies, 2001)

This method was combined with the porous medium approach by Haxaire (1999) and Boulard and Wang (2002) by equating relations (17) and (19). The inertial factor C_f and the permeability K of the porous medium are then deduced from the plant cover characteristics (l_l, C_v) following the relation:

$$\frac{C_f}{K^{0.5}} = l_l C_v \tag{20}$$

The sensible heat and water vapour exchanges. The last step in determining the true microclimatic picture at the plant level involves the modelling of the heat and water vapour exchanges between leaves and air. This can be done by combining the porous medium approach to model dynamic effects and a macro-model of heat and mass transfer between the leaves and the air within each mesh of the crop cover (Haxaire, 1999; Boulard & Wang, 2002). The sink of momentum due to the crop cover and the sensible and latent (crop transpiration) heat exchange between the crop cover and the air should be considered in conjunction with the use of a customised CFD programme (Haxaire, 1999). The exchange of heat and water vapour between leaves and air is described by means of the heat and mass balance of leaves with the air. Each mesh of the crop cover is assimilated to a 'volume heat source' receiving a radiative flux. This flux is partitioned into convective sensible and latent heat fluxes water (Roy *et al.*, 2002) depending on the conductances (stomatal and aerodynamic) between the crop (characterised by its surface temperature) and the air. The partition depends on the heat and water conductance (stomatal and aerodynamic) between the solid matrix and the air within each mesh of the porous medium, the stomatal and aerodynamic conductances are related to the computed local air speed and climatic conditions. Finally, two additional outputs of great interest are available for each mesh of the crop cover: the temperature of the crop surface and the transpiration of the cover. Following this approach, the microclimate and transpiration heterogeneity of a lettuce crop in a tunnel were studied and the results were compared with experimental data (Boulard & Wang, 2002).

4. Conclusions

The scientific literature relative to convection and ventilation processes in greenhouses involving studies of distributed climates has been presented in this review. From the first researches on inside climate in closed empty greenhouses to the recent studies of the climate at the plant and organ level, we have observed a clear development in complexity.

In almost all the cases, the modelling approach is based on the general equations of fluid transfers with either analytical solutions for simple geometrical cases such as the determination of leaf boundary layer climate or, using computer fluid dynamics (CFD), with the discretisation of the equations describing the fluid dynamics of the whole greenhouse domain. Measurement techniques associated with these approaches also present a growing complexity, with the determination of air flow and climate parameter patterns using particle imagery visualisation or sonic anemometry.

Focusing on the study of the distributed climate, it is observed that there is a distinct increase in complexity between the first simulation of a confined model-scale greenhouse by Nara (1979) to the most recent studies of Fatnassi *et al.* (2001b) and Reichrath and Davis (2001) relating to multi-span greenhouses of one hectare or more. Progress in the level of realism has also been made: the first studies concerned only empty greenhouses, whereas the most recent simulations consider the dynamic action of the crop on the flow and the subsequent heat and mass exchanges. Similarly, the effect of various structural elements such as the vents (Lee & Short, 2000) and different insect-proof screens on the flow (Teitel & Schlykar, 1998), and on the inside climate (Fatnassi *et al.*, 2001b), have been taken into account in the first parametric studies.

More generally, there is now the opportunity to call on a large panoply of measurement or modelling techniques giving access to the distributed climate and allowing for its determinism. Considering the specific needs of each type of plant and other biotic agents, it will then be possible to control the climate at plant level with a greater economy of means, matter and energy and a much better efficiency. The use of CFD for improving the greenhouse-crop system is still at the beginning. Combined with other approaches, such as the use of simple analytical solutions for the exploration of climate gradients in the leaf boundary layer, it should lead to significant improvements of greenhouse design and climate control strategies in the near future.

References

Aubinet M; Deltour J (1994). Natural convection above line heat sources in greenhouse canopies. International Journal of Heat and Mass Transfer, **37**(12), 1795–1806

Baille A (1975). Etude de l'influence du positionnement des aérations sur les champs de température et de vitesse à l'intérieur des tunnels de semi-forçage. [Air speed and temperature dependance on the position of the opening surfaces for low tunnels.] Annales Agronomiques, **26**(3), 265–275

Baille M; Baille A; Delmon D (1994). Microclimates and transpiration of greenhouse rose crops. Agricultural and Forest Meteorology, **71,** 83–97

Bakker J C (1986). Measurement of canopy transpiration or evapotranspiration in greenhouse by means of a simple vapour balance model. Agricultural and Forest Meteorology, **37,** 133–141

Bartzanas T; Boulard T; Kittas C (2001). Numerical simulation of the airflow and temperature distribution in a tunnel greenhouse equipped with insect-proof screen in the openings. Computers and Electronics in Agriculture, Special Issue on Applications of CFD in the Agri-food Industry, **34,** 207–221

Bejan A (1984). Convection Heat Transfer. John Wiley & Sons, New York

Bird R B; Stewart W E; Lightfoot E N (1965). Transport Phenomena. John Wiley & Sons, New York

Boulard T; Wang S (2002). Experimental and numerical study on the heterogeneity of crop transpiration in a plastic tunnel. Computers and Electronics in Agriculture, Special Issue on Applications of CFD in the Agri-food Industry, **34,** 173–190

Boulard T; Meneses J F; Mermier M; Papadakis G (1996). The mechanisms involved in the natural ventilation of greenhouses. Agricultural and Forest Meteorology, **79,** 61–77

Boulard T; Papadakis G; Kittas C; Mermier M (1997). Air flow and associated sensible heat exchanges in a naturally ventilated greenhouse. Agricultural and Forest Meteorology, **88,** 111–119

Boulard T; Lamrani M A; Roy J C; Jaffrin A; Bouirden L (1998). Natural ventilation by thermal effect in a one-half scale model mono-span greenhouse. Transactions of the ASAE, **41**(3), 773–781

Boulard T; Haxaire R; Lamrani M A; Roy J C; Jaffrin A (1999). Characterization and modelling of the air fluxes induced by natural ventilation in a greenhouse. Journal of Agricultural Engineering Research, **74,** 135–144

Boulard T; Wang S; Haxaire R (2000). Mean and turbulent air flows and microclimatic patterns in an empty greenhouse tunnel. Agricultural and Forest Meteorology, **100,** 169–181

Boulard T; Mermier M; Fargues J; Smits N; Rougier M; Roy J C (2002). Tomato leaf boundary layer climate: implication for microbiological control of whiteflies in greenhouse. Agricultural and Forest Meteorology, **110,** 159–176

Bradshaw P (1971). An introduction to turbulence and its measurement. Pergamon press, Oxford

Brundrett E (1993). Prediction of pressure drop for incompressible flow through screens. Journal of fluids engineering, **114,** 239–242

Bruse M (1995). Development of a micro-scale model for the calculation of surface temperature in structured terrain. MSc Thesis, Institute for Geography, University of Bochum, Germany

Carpenter W J; Bark L D (1967). Temperature patterns in a greenhouse heating. Florist's Review, **309**(3609), 17–19

Chen Y S; Kim S W (1987). Computation of turbulent flows using an extended k–e model. NASA CR-179204

Cowan I R (1972). Mass and heat transfer in laminar boundary layers with particular references to assimilation and transpiration in leaves. Agricultural Meteorology, **10**, 311–329

De Tourdonnet S; Meynard J M; Lafolie F; Roger-Estrade J; Lagier J; Sebillotte M (2001). Non-uniformity of environmental conditions in greenhouse lettuce production increases the risk of N pollution and lower product quality. Agronomie, **21**(4), 297–310

Fatnassi H; Boulard T; Bouirden L (2001a). Simulation of air flux and temperature patterns in a large scale greenhouse equipped with insect-proof nets. Acta Horticulturae, in press

Fatnassi H; Boulard T; Bouirden L; Sappe G (2001b). Ventilation performances of a large canarian type greenhouse equipped with insect-proof nets. Acta Horticulturae, in press

Favre A; Kovasznay L S G; Dumas R; Gaviglio J; Coantic M (1976). La turbulence en mécanique des fluides. [Turbulence in fluids mechanic.] Gauthier-Villars, Paris

Gray D D; Giorgini A (1976). The validity of the Boussinesq approximation for liquids and gases. International Journal of Heat and Mass Transfer, **19,** 545–551

Green S R (1992). Modelling turbulent air flow in a stand of widely-spaced trees. Phoenics Journal, **3,** 294–295

Harlow F H; Nakayama P I (1967). Turbulence transport equations. Physics of fluids, **10,** 2323

Haxaire R (1999). Caractérisation et Modélisation des écoulements d'air dans une serre. [Characterisation and modelling of air flow in a greenhouse.] Thèse de Docteur en Sciences de l'Ingénieur de l'Université de Nice, Sophia Antipolis. 148pp

Haxaire R; Boulard T; Mermier M (2000). Greenhouse natural ventilation by wind forces. Acta Horticulturae, **534,** 31–40

Hoff S J; Janni K A; Jacobson L D (1992). Three-dimensional buoyant turbulent flows in a scaled model, slot-ventilated, livestock confinement facility. Transactions of the ASAE, **35**(2), 671–686

Jewet T J; Jarvis W R (2001). Management of the greenhouse climate in relation to disease control: a review. Agronomie, **21**(4), 351–366

Kacira M; Short T H; Stowell R R (1998). A CFD evaluation of naturally ventilated, multi-span, sawtooth greenhouses. Transactions of the ASAE, **41**(3), 833–836

Kempes F L K; Van den Braak N J (2000). Heating system position and vertical microclimate distribution in chrysanthemum greenhouse. Agricultural and Forest Meteorology, **104,** 133–142

Kittas C; Boulard T; Bartzanas T; Katsoulas N; Mermier M (2002). Influence of an insect proof screen on ventilation rate in a greenhouse equipped with continuous roof vent. Transactions of the ASAE, in press

Kosmos S R; Riskowski G L; Christianson L L (1993). Force and stativ pressure resulting from airflow through screens. Transaction of the ASAE, **35**(6), 1467–1472

Krauss G; Depecker P; Kindagen J I (1997). Méthode des réseaux de neurones pour le calcul des coefficients de vitesse, Application aux écoulements de l'air dans les bâtiments. [Neural networks for estimating air speed coefficients: application to air flow studies in buildings.] Revue Générale érale de Thermique, **36,** 180–191

Lam C K J; Bremhorst K A (1981). Modified form of the k–e model for predicting wall turbulence. Journal of Fluids Engineering, **103,** 456–460

Lamrani M A (1997). Caractérisation et modélisation de la convection naturelle laminaire et turbulente à l'intérieur d'une serre. [Characterisation and modelling of laminar and turbulent natural convection in greenhouses.] Thèse de Doctorat, Université d'Agadir, Maroc. 160pp

Lamrani M A; Boulard T; Roy J C; Jaffrin A (2001). Airflows and temperature patterns induced in a confined greenhouse. Journal of Agricultural Engineering Research, **78,** 75–88

Launder B E; Spalding D B (1972). Mathematical models of turbulence. Academic press, New York

Lee I; Short T H (2000). Two-dimensional numerical simulation of natural ventilation in a multi-span greenhouse. Transactions of the ASAE, **43**(3), 745–753

Miguel A F; Van den Braak N J; Bot G P A (1997). Analysis of the air flow characteristics of greenhouse screening materials. Journal of Agricultural Engineering Research, **67,** 105–112

Miguel A F; Van de Braak N J; Silva A M; Bot G P A (1998). Free convection heat transfer in screened greenhouse. Journal of Agricultural Engineering Research, **69,** 133–139

Mistriotis A; Arcidiacono C; Picuno P; Bot G P A; Scarascia-Mugnozza G (1997a). Computational analysis of ventilation in greenhouses at zero- and low-wind-speeds. Agricultural and Forest Meteorology, **88,** 121–135

Mistriotis A; Bot G P A; Picuno P; Scarascia-Mugnozza G (1997b). Analysis of the efficiency of greenhouse ventilation using computational fluid dynamics. Agricultural and Forest Meteorology, **85,** 217–228

Montero J I; Munoz P; Anton A (1997). Discharge coefficient of greenhouse windows with insect proof screens. Acta Horticulturae, **443,** 71–77

Montero J I; Hunt G R; Kamarudddin R; Anton A; Bailey B J (2001a). Effect of ventilator configuration on wind driven ventilation in a crop protection structure for the tropics. Journal of Agricultural Engineering Research, **80**(1), 99–107

Montero J I; Anton A; Kamarudddin R; Bailey B J (2001b). Analysis of thermally driven ventilation in tunnel greenhouses using small scale models. Journal of Agricultural Engineering Research, **79**(2), 213–222

Nara M (1979). Studies on air distribution in farm buildings—two dimensional numerical and experiment. Journal of the Society of Agricultural Structures, **9**(2), 18–25

Nield D A; Bejan A (1992). Convection in porous media. Springer-Verlag, New York.

Oca J; Montero J I; Anton A; Crespo D (1998). A method for studying natural ventilation by thermal effects in a tunnel greenhouse using laboratory-scale models. Journal of Agricultural Engineering Research, **72,** 93–104

Okushima L; Sase S; Maekawa T; Ikeguchi A (1998). Airflow patterns forced by wind effect in a venlo type greenhouse. Journal of the Society of Agricultural Structures, **29**(3), 59–68

Parkhurst D F; Duncan P R; Gates D M; Kreith F (1968). Wind-tunnel modelling of convection of heat between air and broad leaves on plants. Agricultural Meteorology, **5,** 33–47

Pearson CC; Owens JE (1992). The resistance to air flow of farm building ventilation components. Journal of Agricultural Engineering Research, **57,** 53–65

Pollet S; Bleyaert P (2000). Application of the Penman-Monteith model to calculate the evapotranspiration of head lettuce in glasshouse conditions. Acta Horticulturae, **519,** 151–161

Reichrath S; Davies T W (2001). Using CFD to model the internal climate of greenhouses: past, present and future. Agronomie, **22,** 3–19

Roy J C; Bailly Y; Boulard T; Haxaire R (2000a). Etude expérimentale de la convection naturelle dans une serre chauffée. [Experimental study on natural convection in an heated greenhouse.] Congrès de la Société Française des Thermiciens. Lyon, France

Roy J C; Bailly Y; Boulard T (2000b). Characterisation of the natural convection in a heated greenhouse. 9th International Symposium on Flow Visualization, Edinburgh, UK, Paper 254

Roy J C; Boulard T; Kittas C; Wang S (2002). Convective and ventilation transfers in greenhouses, Part 1: Greenhouse considered as a perfectly stirred tank. Biosystems Engineering, **83,** 1–20, doi: 10.1006/bioe.2002.0107.

Sase S (1989). The effect of plant arrangement on airflow characteristics in a naturally ventilated glasshouse. Acta Horticulturae, **245,** 429–435

Sase S; Takakura T; Nara M (1984). Wind tunnel testing on airflow and temperature distribution of a naturally ventilated greenhouse. Acta Horticulturae, **148,** 329–336

Schlichting H (1955). Boundary-layer theory. Mc Graw-Hill, New York.

Schuepp P H (1993). Tansley review no. 59. Leaf boundary layers. New Phytologist, **125,** 477–507

Seginer I; Boulard T; Bailey B J (1994). Neural network model of greenhouse climate. Journal of Agricultural Engineering Research, **59,** 203–216

Stanghellini C (1987). Transpiration of greenhouse crops: an aid to climate management. PhD Thesis, Agricultural University of Wageningen, The Netherlands, 150pp

Teitel M (2001). The effect of insect-proof screens in roof openings on greenhouse microclimate. Agricultural and Forest Meteorology, **2989,** 1–13

Teitel M; Shlykar A (1998). Pressure drop across insect-proof screens. Transaction of the ASAE, **41**(6), 1829–1834

Tennekes H; Lumley J L (1972). A first course in turbulence. MIT Press, Cambridge

Thom A S (1971). Momentum absorption by vegetation. Quarterly Journal of Royal Meteorology Society, **97,** 414–428

Wang S (1998). Measurement and modelling of natural ventilation in a large scale Venlo-type greenhouse. PhD Thesis, Gembloux, Belgium, 194pp

Wang S; Deltour J (1999). Airflow patterns and associated ventilation function in large-scale multi-span greenhouses. Transactions of the ASAE, **42**(5), 1409–1414

Wang S; Boulard T; Haxaire R (1999). Air speed profiles in a naturally ventilated greenhouse with a tomato crop. Agricultural and Forest Meteorology, **96,** 181–188

Yakhot V; Orszag S A (1986). Renormalization group analysis of turbulence. Journal of Scientific Computing, 1.3

Yang X; Short T H; Fox R D; Bauerle W L (1990). Dynamic modeling of the microclimate of a greenhouse cucumber row-crop, Part 2: validation and simulation. Transactions of the ASAE, **33**(5), 1710–1716

Zhao Y; Teitel M; Barak M (2001). Vertical temperature and humidity gradients in a naturally ventilated greenhouse. Journal of Agricultural Engineering Research, **78**(4), 431–436